Asian Journal of Chemistry; Vol. 37, No. 10 (2025), 2426-2430
ASIAN JOURNAL OF CHEMISTRY
https://doi.org/10.14233/ajchem.2025.34358

Carbon Dot Functionalized with Hematite for Hydrogen Evolution

SONI TYAGI, SOUMITA TALUKDAR*, and AMAN REHAN

School of Engineering & Sciences, G.D. Goenka University, Gurugram-122103, India

*Corresponding author: Email: soumita.talukdar@gdgu.org

Received: 27 June 2025 *Accepted*: 8 September 2025 *Published online*: 30 September 2025 AJC-22126

Carbon dots (CDs) are promising photocatalysts that have attracted attention due to their property of surface functionalization, low-cost facile scale-up synthesis, magnificent electron transfer efficiency and tunable light harvesting range photostability, photoluminescence properties and low cost. Whereas hematite can degrade pollutants through photocatalysis efficiently, exhibiting Fenton and photo-Fenton oxidations and due to their magnetic properties suspended solids can easily be separated with magnetic separation techniques. CDs prepared using green carbon sources such as waste tea leaves by microwave treatment method. Hematite-coated CD-based nanocomposite can be developed for highly efficient photocatalysis with enhanced surface area, desirable band structure and ease of separation. The nanocomposite CDs@Fe_2O_3 synthesized using waste carbon sources. CDs@Fe_2O_3 nanocomposites were effectively developed in this study using straightforward hydrothermal process in single pot and used as efficient photocatalyst for hydrogen evolution reaction (HER) under visible light irradiation. One of the most promising fuel options is hydrogen, a clean and renewable energy source. The nanocomposite exhibited an efficient photocatalyst for the evolution of 1300 µmol g^{-1} of H_2 in 4 h.

Keywords: Photocatalyst, Hematite, Carbon dots.

INTRODUCTION

Carbon dots (CDs) have garnered significant interest and emerged as a novel category of fluorescent nanomaterials owing to their exceptional characteristics including encompassing optical and electronic properties, non-toxicity and affordability. CDs, characterized by their size of less than 10 nm, belong to the category of zero-dimensional quantum dots. These nanoparticles are commonly perceived as quasi-zero-dimensional entities and fragments derived from graphene sheets [1]. The optical and biological characteristics of CDs are contingent upon the distinct synthesis approaches employed and the surface functionalization applied to them. By precisely controlling synthesis conditions and surface functionalization, carbon dots can exhibit tunable fluorescence and exceptional biocompatibility [2]. Carbon dots also exhibit considerable potential in the realms of bioimaging and drug delivery, attributed to their minimal toxicity, favourable biocompatibility and adjustable fluorescence [3]. These attributes enable the tracking and imaging of biological structures and processes with precision and efficacy [4].

A number of studies have recently concentrated on using electrocatalytic water splitting for produce H_2 gas. Efficient electrocatalysts are needed for this straightforward and effective process of electrocatalytic water splitting [5]. The clean nature of photocatalysis, combined with its ability to harness virtually limitless solar energy, makes it a promising sustainable technology that minimizes environmental impact [6]. Usually semiconductors, photocatalysts are able to be activated by light irradiation to produce charge carriers of reductive electrons and highly oxidative holes for various redox processes. The most promising choices have been thought to be II–VI group quantum dots (QDs) and Cd-free I–III-VI QDs due to their exceptional optical qualities, huge surface area and special quantum confinement effect [7,8]. Since QDs have attracted significant interest in photocatalysis due to their composition-dependent tunable band gaps [9] but several conventional QDs suffer from poor stability and limited synthesis efficiency, which restrict their practical applications. In contrast, CDs, prepared from organic semiconductor nanomaterials, generate photoinduced electron-hole pairs upon solar light irradiation, offering enhanced photocatalytic performance

and improved stability [10,11]. Furthermore, CDs are an essential energy shuttle medium as they may function as electron donors and acceptors in suspension or solution [12]. As a result, CDs are widely utilized in photocatalysis to produce hydrogen [13].

It is also reported that hematite serves as a potential photocatalyst for H_2 production. Favourable properties such as abundance, photochemical stability, eco-friendliness, cost-effective efficient, suitable band gap and the ability to achieve a theoretical maximum solar-to-hydrogen efficiency of 15.4% [14,15]. In this work, waste tea extract is used to stabilize and stimulate the formation of CDs@hematite nanocomposite as photocatalysts for H_2 evolution.

EXPERIMENTAL

Mostly chemicals and reagents were procured from CDH, India whereas ammonia solution from Molychem, India. Waste tea leaves and a microwave from Haier were used for the synthesis of carbon dots. REMI R-8C was used for centrifuge and Fluoromax for photoluminescence.

Synthesis of CDs@Fe_2O_3 nanocomposite: A 2 g of waste tea leaf powder was dispersed in 100 mL of distilled water and subjected to microwave irradiation at 180 ºC for 4 min. Then, the yellowish-brown CDs suspension was first mixed with $FeSO_4$ solution and subjected to magnetic stirring. Subsequently, 0.8 g of $FeCl_3$ was added and the mixture was stirred continuously for 30 min. Finally, 7 mL of ammonia solution was introduced gradually until the pH of the mixture reached 10. The black precipitate was centrifuged and kept in the oven for drying overnight.

Photocatalytic H_2 evolution: Photocatalytic hydrogen evolution experiments were conducted in a 100 mL double-walled Pyrex photoreactor equipped with an airtight rubber septum. A 10 mg of catalyst was uniformly dispersed in 20 mL of an aqueous solution containing 2 mL of methanol, which served as a sacrificial electron donor (SED). To ensure an inert atmosphere, the solution was degassed and purged with N_2 gas. Irradiation was carried out using a 420 W xenon lamp (Newport Co., Ltd., USA) with an intensity of 0.19 W cm^{-2}, equipped with a cut-off filter ($\lambda > 420$ nm). The rate of hydrogen evolution was monitored every hour for 4 h using a Perkin-Elmer Clarus 590 gas chromatograph (GC) fitted with a molecular sieve 5 Å column and a thermal conductivity detector (TCD), with nitrogen as the carrier gas.

RESULTS AND DISCUSSION

XRD studies: The XRD pattern of CDs@Fe_2O_3 derived from waste tea leaves exhibits a small peak at $2\theta = 23.16^o$ confirming the presence of CDs, along with the peaks at $2\theta = 32.67^o$, $2\theta = 35.44^o$ [16] and 62.55^o that of Fe_2O_3 NPs, which is well accordance with spinel structure of (JCPDS98-3969) [17]. In addition, some peaks near 46.54^o are easily attributed to (331) (Fig. 1). This suggests a relationship between these peaks and Fe_2O_3 of (JCPD card no. 98-0625) [16]. The small and broad peak observed for the CDs is attributed to their amorphous nature and smaller particle size compared to Fe_2O_3 nanoparticles. The crystallite size of the green synthesized

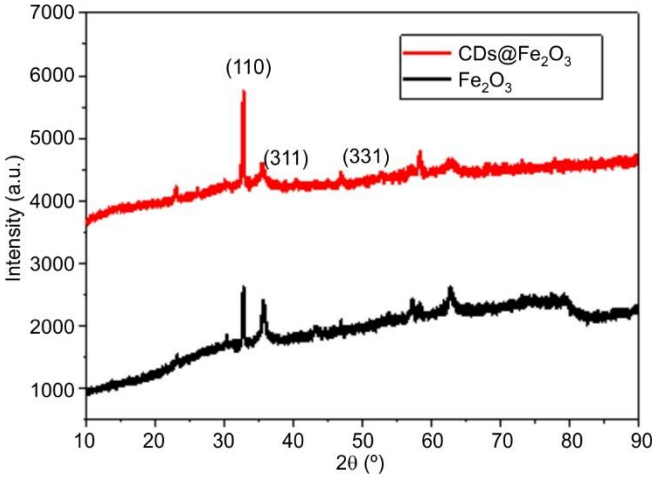

Fig. 1. XRD spectra of prepared CDs@hematite with waste tea and orange peel. Characteristic broad peak of CD was observed at $2\theta = 23.16^o$ along with Fe_2O_3 peaks at 32.67^o and 35.44^o

nanocomposite was also evaluated using Debye-Scherrer equation:

$$\text{Crystallite size (D)} = \frac{k\lambda}{\beta \cos\theta} \quad (1)$$

where D = crystallite size; k = Scherrer constant (0.98), λ = wavelength of the X-ray source (1.94 Å of Cu), β = FWHM of the most intense peak and θ = angle of the most intense peak.

Thus, the crystallite size (D) of the nanocomposite was calculated to be 1.36 nm.

Optical studies: UV-Vis spectra of CDs@Fe_2O_3 nanocomposite with strong green luminescence under UV light indicating excellent optical properties. The UV-Vis absorption spectrum showed peaks at approximately 205 nm and 273 nm, corresponding to the π–π^* transition of C=C bonds and the n–π^* transition of C=O bonds, respectively. These features were formed during the microwave irradiation process used in the synthesis of CDs (Fig. 2).

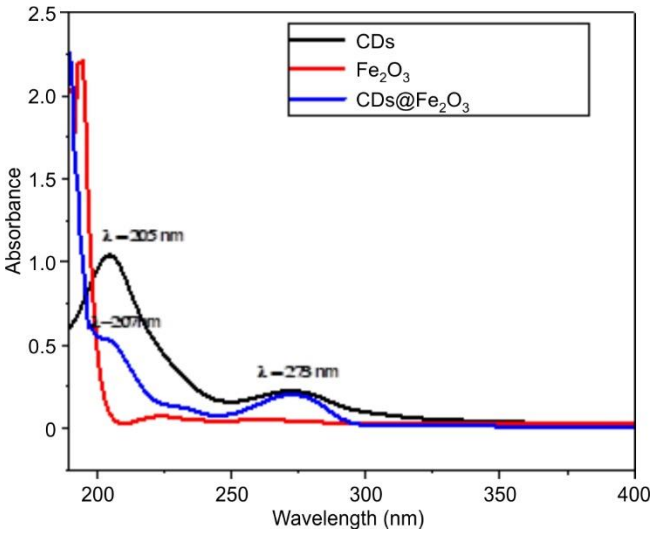

Fig. 2. UV-vis spectra of prepared CDs and CDs@nanocomposites

The photoluminescence (PL) spectra of CDs and CDs@Fe_2O_3 nanocomposite under various excitation wavelengths

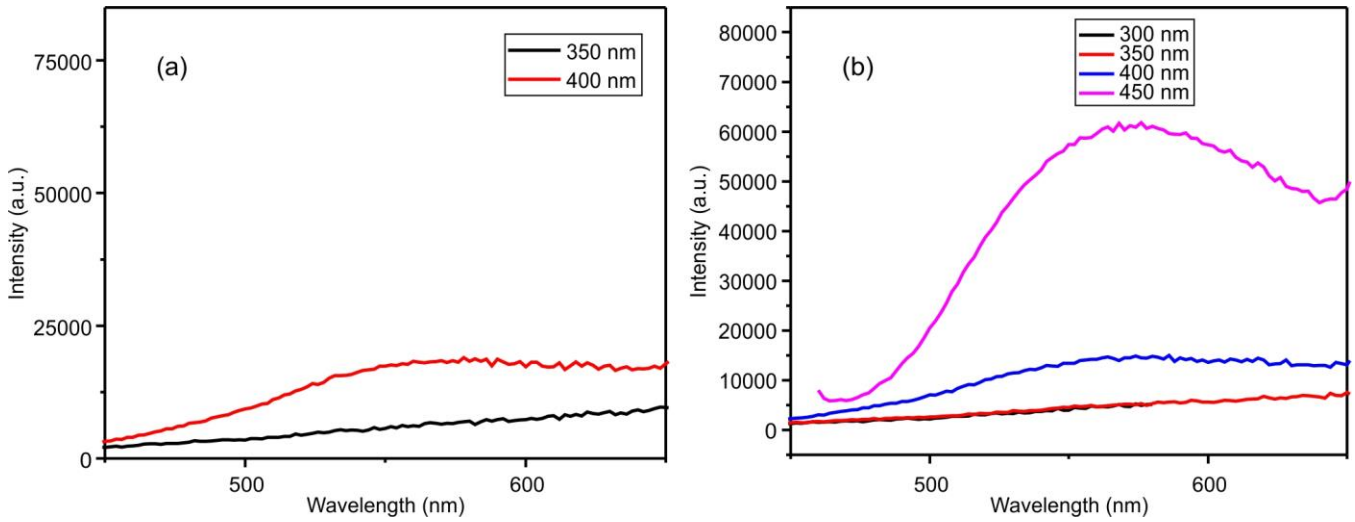

Fig. 3. PL spectra of (a) CDs and (b) CDs@Fe_2O_3

from 300 nm to 460 nm were examined. The wide excitation range of PL measurements indicates the maximum fluorescence emission is around 580 nm with an excitation wavelength of 450 nm (Fig. 3) [1]. The origin of the PL of CDs has been assigned to several reasons such as size (quantum effect), defect, surface groups and passivation and the recombination of electron-hole pairs localized within sp^2 carbon embedded in a sp^3 matrix [18]. The optical absorption is related to π-plasmon transitions in the core of the dots [19] while the fluorescence emissions in the visible to near-IR are due to the photogenerated electrons and holes trapped at various surface sites and their associated radiative recombination [20].

FTIR spectral studies: The FTIR spectra of both CDs and CDs@Fe_2O_3 nanocomposite are shown in Fig. 4. The absorption band observed in the range of 600–400 cm^{-1} corresponds to the Fe–O stretching vibrations, confirming the presence of iron oxide in the nanocomposite. Additional bands approximately at 850 cm^{-1} and 930 cm^{-1} are attributed to the C–O stretching vibrations, which are not present in the spectra of pure CDs sample. Furthermore, magnetic Fe_2O_3 nanoparticles exhibit a characteristic broad band centered around 632 cm^{-1}, further supporting the successful incorporation of iron oxide [21].

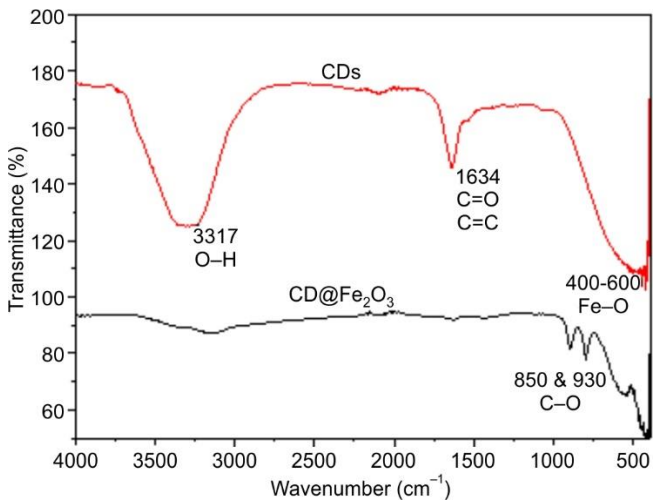

Fig. 4. FTIR spectra of CDs & CDs@Fe_2O_3

Morphological studies: Figs. 5 and 6 represent the morphological characterization of the CDs@ Fe_2O_3 nanocomposite using scanning electron microscopy (SEM) and transmission electron microscopy (TEM), respectively. The images reveal a relatively spherical uniform shape and consistent morphology; however, some degree of particle aggregation is observed, likely due to the inherent agglomeration tendency of the fine nanocomposites. Furthermore, EDX analysis (Fig. 5b) confirms the presence of carbon (C), oxygen (O), and iron (Fe), confirming the successful formation of the nanocomposite.

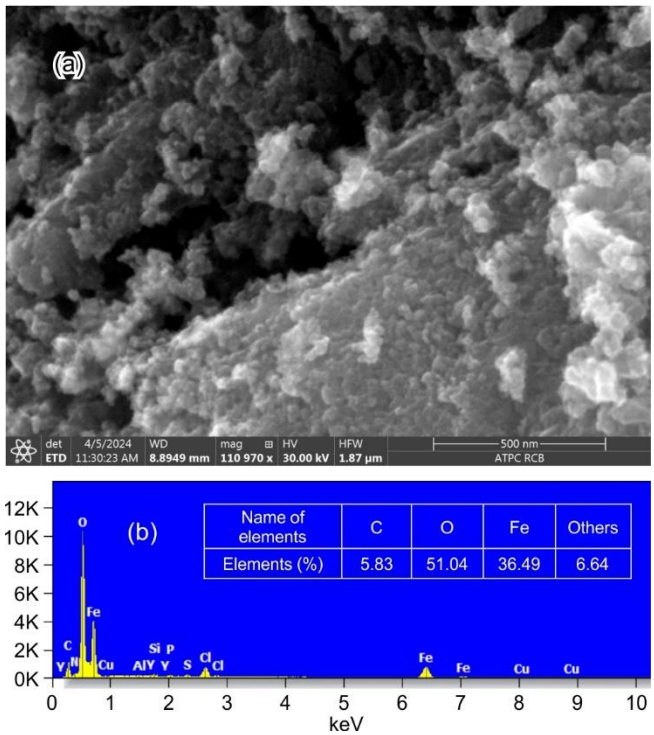

Fig. 5. (a) SEM image of CDs@hematite and (b) EDAX of CDs@Fe_2O_3

The agglomeration observed is likely due to the ultrafine particle size of green synthesized nanocomposite and inhe-

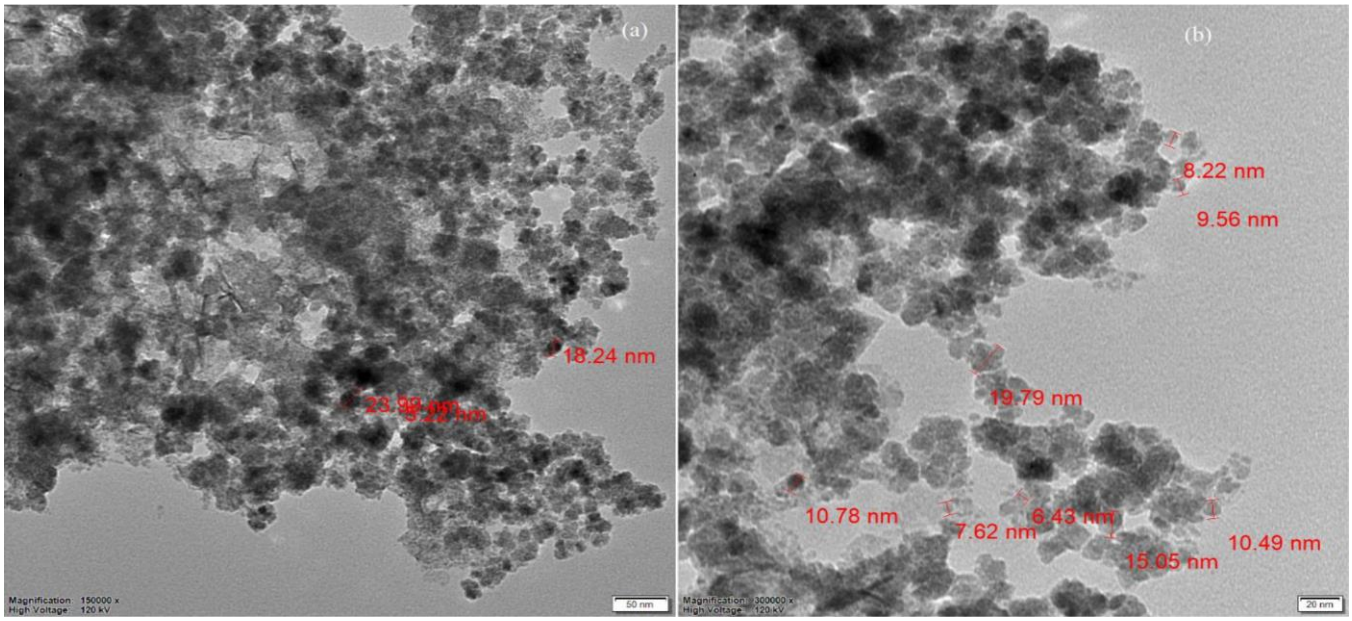

Fig. 6. TEM images of CDs@hematite NC at (a) 50 nm and (b) 20 nm scale

rent magnetic properties, which facilitate strong interparticle attractions [22]. The nanocomposite sizes varied between 12-16 nm, with an average size of 13.5 ± 3.7 nm. The form and size resembled those of the green-synthesized nanocomposite prepared from extract from seaweed [23].

Photocatalytic H_2 evolution: The H_2 evolution in the presence of visible light Xe lamp ($\lambda > 420$ nm) source was observed to yield 1300 μmol g^{-1} in 4 h (Fig. 7). It has been observed that the H_2 evolution was linear in the first 90 min, which then exponentially increased with time, then gradually slowed down that can be attributed to the limitations of the available surface area of the photocatalyst.

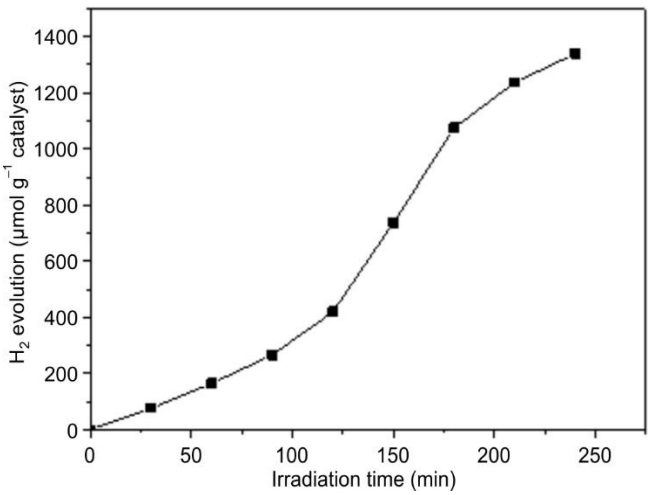

Fig. 7. Evolution of hydrogen by CDs@Fe_2O_3

The mechanism of the H_2 evolution involves visible light absorption by the CD@Fe_2O_3 nanocomposite photocatalyst, generating electrons and holes. The sacrificial agent MeOH donates electrons to these photo-generated holes inhibiting the recombination of the e-h pair, which is finally transferred to water at the active site, for reduction, facilitating the hydrogen evolution reaction (HER) [24]. The schematic of the photocatalytic charge transfer of H_2 evolution by CDs@Fe_2O_3 nanocomposite is shown in **Scheme-I**.

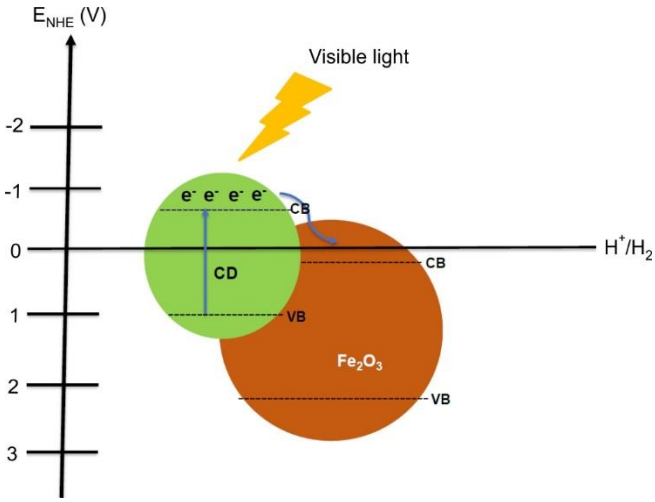

Scheme-I: Photocatalytic charge transfer of H_2 evolution by CDs@Fe_2O_3

Conclusion

In conclusion, CDs@Fe_2O_3 nanocomposite was successfully synthesized *via* a microwave-assisted method utilizing a green extract derived from waste tea leaves and charactered with UV, PL, SEM, TEM, EDX, XRD and FTIR techniques. In the context of photocatalytic hydrogen evolution, the electrode demonstrated enhanced electrocatalytic activity when CDs@$Fe_2O_3$was utilized as the hydrogen evolution reaction (HER) catalyst. Additionally, a synergistic effect between evenly distributed Fe_2O_3 nanoparticles and carbon dots can be achieved, resulting in exceptional long-term stability of CDs@Fe_2O_3. These results might offer a method for quickly creating durable and highly effective nanohybrid catalysts for use in the renewable energy applications.

ACKNOWLEDGEMENTS

The authors would like to express their sincere gratitude to Dr. Sarita Tyagi for her technical support in this article.

CONFLICT OF INTEREST

The authors declare that there is no conflict of interests regarding the publication of this article.

REFERENCES

1. S. Ahmadian-Fard-Fini, M. Salavati-Niasari and D. Ghanbari, *Spectrochim. Acta A Mol. Biomol. Spectrosc.*, **203**, 481 (2018); https://doi.org/10.1016/j.saa.2018.06.021
2. Y. Wang, Y. Zhu, S. Yu and C. Jiang, *RSC Adv.*, 7, 40973 (2017); https://doi.org/10.1039/C7RA07573A
3. W. Su, H. Wu, H. Xu, Y. Zhang, Y. Li, X. Li and L. Fan, *Mater. Chem. Front.*, **4**, 821 (2020); https://doi.org/10.1039/C9QM00658C
4. M. Bartkowski, Y. Zhou, M.N.A. Mustafa, A.J. Eustace and S. Giordani, *Chem. Eur. J.*, **30**, e202303982 (2024); https://doi.org/10.1002/chem.202303982
5. R. Atchudan, T.N.J. Immanuel Edison, S. Perumal, R. Vinodh, N. Muthuchamy and Y.R. Lee, *Fuel*, **277**, 118235 (2020); https://doi.org/10.1016/j.fuel.2020.118235
6. Y. Yao, H. Zhang, K. Hu, G. Nie, Y. Yang, Y. Wang, X. Duan and S. Wang, *J. Environ. Chem. Eng.*, **10**, 107336 (2022); https://doi.org/10.1016/j.jece.2022.107336
7. S. Jain, S. Bharti, G.K. Bhullar and S.K. Tripathi, *J. Lumin.*, **219**, 116912 (2020); https://doi.org/10.1016/j.jlumin.2019.116912
8. Y. Liu, F. Li, H. Huang, B. Mao, Y. Liu and Z. Kang, *J. Semicond.*, **41**, 091701 (2020); https://doi.org/10.1088/1674-4926/41/9/091701
9. F. Li, Y. Liu, B. Mao, L. Li, H. Huang, D. Zhang, W. Dong, Z. Kang and W. Shi, *Appl. Catal. B*, **292**, 120154 (2021); https://doi.org/10.1016/j.apcatb.2021.120154
10. H. Jung, V. S. Sapner, A. Adhikari, B. R. Sathe and R. Patel, *Front. Chem.*, **10**, 881495 (2022); https://doi.org/10.3389/fchem.2022.881495
11. N. Ullal, K. Muthamma, and D. Sunil, *Chem. Pap.*, **76**, 6097 (2022); https://doi.org/10.1007/s11696-022-02353-3
12. T. Wang, C. Nie, Z. Ao, S. Wang and T. An, *J. Mater. Chem. A Mater. Energy Sustain.*, **8**, 485 (2020); https://doi.org/10.1039/C9TA11368A
13. L. Cheng, Q. Xiang, Y. Liao and H. Zhang, *Energy Environ. Sci.*, **11**, 1362 (2018); https://doi.org/10.1039/C7EE03640J
14. B.K. Jha, S. Chaule and J.-H. Jang, *Mater. Chem. Front.*, **8**, 2197 (2024); https://doi.org/10.1039/D3QM01100C
15. Z. Najaf, D.L.T. Nguyen, S.Y. Chae, O.-S. Joo, A.U.H.A. Shah, D.-V.N. Vo, V.-H. Nguyen, Q.V. Le and G. Rahman, *Int. J. Hydrogen Energy*, **46**, 23334 (2021); https://doi.org/10.1016/j.ijhydene.2020.07.111
16. Z.I. Takai, M.K. Mustafa and S. Asman, *Asian J. Chem.*, **30**, 2625 (2018); https://doi.org/10.14233/ajchem.2018.21473
17. S. Shafiee, O. Akhavan, H. Hatami, and P. Hoseinkhani, **53**, 804 (2015).
18. W. You, W. Zou, S. Jiang, J. Zhang, Y. Ge, G. Lu, D.W. Bahnemann and J.H. Pan, *Carbon Neutralization*, **3**, 245 (2024); https://doi.org/10.1002/cnl2.120
19. H. Safardoust-Hojaghan, M. Salavati-Niasari, O. Amiri and M. Hassanpour, *J. Mol. Liq.*, **241**, 1114 (2017); https://doi.org/10.1016/j.molliq.2017.06.106
20. S. Ahmadian-Fard-Fini, M. Salavati-Niasari and H. Safardoust-Hojaghan, *J. Mater. Sci. Mater. Electron.*, **28**, 16205 (2017); https://doi.org/10.1007/s10854-017-7522-1
21. S. Zhu, J. Guo, J. Dong, Z. Cui, T. Lu, C. Zhu, D. Zhang and J. Ma, *Ultrason. Sonochem.*, **20**, 872 (2013); https://doi.org/10.1016/j.ultsonch.2012.12.001
22. M.B. Gawande, A.K. Rathi, I.D. Nogueira, R.S. Varma and P.S. Branco, *Green Chem.*, **15**, 1895 (2013); https://doi.org/10.1039/c3gc40457a
23. Y.P. Yew, K. Shameli, M. Miyake, N. Kuwano, N.B. Bt Ahmad Khairudin, S.E. Bt Mohamad and K.X. Lee, *Nanoscale Res. Lett.*, **11**, 276 (2016); https://doi.org/10.1186/s11671-016-1498-2
24. N. Gupta, S.M. Gupta and S.K. Sharma, *Carbon Lett.*, **29**, 419 (2019); https://doi.org/10.1007/s42823-019-00068-2